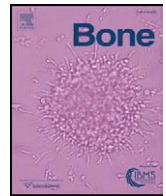




Contents lists available at ScienceDirect

Bone

journal homepage: [www.elsevier.com/locate/bone](http://www.elsevier.com/locate/bone)

## Decreased osteoclastogenesis and high bone mass in mice with impaired insulin clearance due to liver-specific inactivation to CEACAM1

S. Huang<sup>a</sup>, M. Kaw<sup>a,d</sup>, M.T. Harris<sup>a,1</sup>, N. Ebraheim<sup>a</sup>, M.F. McInerney<sup>c,d</sup>, S.M. Najjar<sup>b,d</sup>, B. Lecka-Czernik<sup>a,b,d,\*</sup>

<sup>a</sup> Department of Orthopaedic Surgery, MS 1008, University of Toledo Medical Center, 3000 Arlington Ave., Toledo, OH 43614, USA

<sup>b</sup> Department of Physiology and Pharmacology, MS 1008, University of Toledo Medical Center, 3000 Arlington Ave., Toledo, OH 43614, USA

<sup>c</sup> Department of Medicinal and Biological Chemistry, MS 1008, University of Toledo Medical Center, 3000 Arlington Ave., Toledo, OH 43614, USA

<sup>d</sup> Center for Diabetes and Endocrine Research, MS 1008, University of Toledo Medical Center, 3000 Arlington Ave., Toledo, OH 43614, USA

### ARTICLE INFO

#### Article history:

Received 4 August 2009

Revised 17 December 2009

Accepted 19 December 2009

Available online xxx

Edited by: J. Aubin

#### Keywords:

CEACAM1

Insulin

Bone

Remodeling

Osteoclast

### ABSTRACT

Type 2 diabetes is associated with normal-to-higher bone mineral density (BMD) and increased rate of fracture. Hyperinsulinemia and hyperglycemia may affect bone mass and quality in the diabetic skeleton. In order to dissect the effect of hyperinsulinemia from the hyperglycemic impact on bone homeostasis, we have analyzed L-SACC1 mice, a murine model of impaired insulin clearance in liver causing hyperinsulinemia and insulin resistance without fasting hyperglycemia. Adult L-SACC1 mice exhibit significantly higher trabecular and cortical bone mass, attenuated bone formation as measured by dynamic histomorphometry, and reduced number of osteoclasts. Serum levels of bone formation (BALP) and bone resorption markers (TRAP5b and CTX) are decreased by approximately 50%. The L-SACC1 mutation in the liver affects myeloid cell lineage allocation in the bone marrow: the (CD3<sup>-</sup>CD11b<sup>-</sup>CD45R<sup>-</sup>) population of osteoclast progenitors is decreased by 40% and the number of (CD3<sup>-</sup>CD11b<sup>-</sup>CD45R<sup>+</sup>) B-cell progenitors is increased by 60%. L-SACC1 osteoclasts express lower levels of c-fos and RANK and their differentiation is impaired. *In vitro* analysis corroborated a negative effect of insulin on osteoclast recruitment, maturation and the expression levels of c-fos and RANK transcripts. Although bone formation is decreased in L-SACC1 mice, the differentiation potential and expression of the osteoblast-specific gene markers in L-SACC1-derived mesenchymal stem cells (MSC) remain unchanged as compared to the WT. Interestingly, however, MSC from L-SACC1 mice exhibit increased PPAR $\gamma$ 2 and decreased IGF-1 transcript levels. These data suggest that high bone mass in L-SACC1 animals results, at least in part, from a negative regulatory effect of insulin on bone resorption and formation, which leads to decreased bone turnover. Because low bone turnover contributes to decreased bone quality and an increased incidence of fractures, studies on L-SACC1 mice may advance our understanding of altered bone homeostasis in type 2 diabetes.

© 2010 Published by Elsevier Inc.

### Introduction

Patients with type 2 diabetes mellitus (T2DM) exhibit normal-to-higher bone mineral density (BMD) than nondiabetics. Despite higher BMD, T2DM patients are at a 2-fold higher risk for fracture [8]. This suggests that instead of bone mass, diabetes-related factors are essential determinants of bone quality and increased fracture risk.

Hyperglycemia and hyperinsulinemia are cardinal features of insulin resistance in T2DM and insulin appears to have an anabolic effect on bone [21]. *In vitro* analyses have shown that insulin decreases the resorptive activity in osteoclasts, but stimulates proliferation and differentiation while inhibiting apoptosis in osteoblasts [4,20,21]. Insulin action on bone may involve direct signaling through the insulin receptor, activation of bone anabolic IGF-1 signaling by binding to IGF-1 receptor, or synergistic effects with other anabolic agents such as parathyroid hormone (PTH) [21,24]. Most of the studies on the effect of insulin on bone are based on *in vitro* models. Available *in vivo* models of altered insulin metabolism are usually in the context of either high glucose levels or changes in the growth hormone/IGF-1 signaling axes, which may confound the effect of insulin on bone.

The carcinoembryonic antigen-related cell adhesion molecule 1 (CEACAM1) is a transmembrane glycoprotein belonging to the immunoglobulin superfamily [10]. The CEACAM1 regulates insulin action by promoting insulin clearance [5,15,25]. The CEACAM1

\* Corresponding author. Department of Orthopaedic Surgery, MS 1008, University of Toledo Medical Center, 3000 Arlington Ave., Toledo, OH 43614, USA. Fax: +1 419 383 2871.

E-mail addresses: [shilong.huang@utoledo.edu](mailto:shilong.huang@utoledo.edu) (S. Huang), [meenakshi.kaw@utoledo.edu](mailto:meenakshi.kaw@utoledo.edu) (M. Kaw), [mtharris@umich.edu](mailto:mtharris@umich.edu) (M.T. Harris), [nabil.ebraheim@utoledo.edu](mailto:nabil.ebraheim@utoledo.edu) (N. Ebraheim), [marcia.mcinerney@utoledo.edu](mailto:marcia.mcinerney@utoledo.edu) (M.F. McInerney), [sonia.najjar@utoledo.edu](mailto:sonia.najjar@utoledo.edu) (S.M. Najjar), [beata.leckaczernik@utoledo.edu](mailto:beata.leckaczernik@utoledo.edu) (B. Lecka-Czernik).

<sup>1</sup> Current address: Department of Biomedical Engineering, University of Michigan, Ann Arbor, MI 48105, USA.

C-terminal serine (S503) is a substrate for the insulin receptor tyrosine kinase and a regulator of receptor-mediated insulin endocytosis and its degradation. The dominant negative S503A mutation prevents CEACAM1 phosphorylation and affects insulin clearance. Transgenic L-SACC1 animals overexpress CEACAM1(S503A) specifically in the liver [17]. The L-SACC1 mouse exhibits hyperinsulinemia and glucose intolerance, due to impairment of hepatic insulin clearance [16]. Moreover, L-SACC1 mice have increased visceral adiposity with associated macrophage infiltration. The mice do not develop overt diabetes, as assessed by normal fasting glucose levels. Thus, we, herein, used the L-SACC1 mouse to investigate whether elevations in insulin levels cause an increase in bone mass and alter bone cell phenotype in the absence of altered glucose levels.

## Materials and methods

### Animals

Transgenic L-SACC1 mice were generated as previously described [17]. Animals were housed on 12-h dark/light cycle and fed standard chow and water ad libitum. All procedures were approved by the University of Toledo Health Science Campus Institutional Animal Care and Utilization Committee. Only male animals were used in presented experiments. To permit dynamic bone histomorphometry, mice were injected ip with 30 µg/g body weight of tetracycline 7 and 2 days before sacrifice. Animals were euthanized by CO<sub>2</sub> inhalation and cervical dislocation. Weights of epididymal fat corresponding to white adipose tissue (WAT) and interscapular fat corresponding to brown adipose tissue (BAT) were recorded. Bone marrow was harvested from both femora. Right tibia and L5 vertebrae were analyzed using micro-computed tomography (mCT), whereas left tibia was decalcified and embedded in paraffin for histological assessment. After mCT, the right tibiae were embedded undecalcified in methyl methacrylate and analyzed for dynamic histomorphometry at the Center for Orthopaedic Research, University of Arkansas for Medical Sciences (Little Rock, AR), as previously described [11].

### Measurements of metabolic serum parameters

Animals were fasted for 18 h and serum samples were prepared from blood collected by cardiac puncture immediately after euthanasia. Serum insulin levels and IGF-1 levels were measured using immunoassays provided by ALPCO Diagnostics (Salem, NH) and MECORE Laboratory (Bangor, ME), respectively. Bone-specific alkaline phosphatase was measured colorimetrically using the Alkaline Phosphatase Diagnostic Kit (Sigma-Aldrich, St. Louis, MO) in the presence of L-glucosamine to exclude muscle and liver enzymatic activity. N-terminal propeptide of type I procollagen (P1NP), C-terminal telopeptide of type I collagen (CTX), and tartrate-resistant acid phosphatase form 5b (TRAP5b) were measured using diagnostic kits provided by Immunodiagnostic Systems Inc. (IDS, Scottsdale, AZ).

### Micro-computed tomography analysis

mCT analysis was performed using a SCANCO µCT35 (SCANCO Medical AG, Bassersdorf, Switzerland) equipped with a 10-mm focal spot microfocus x-ray tube. Scans were performed at the following instrument settings: E = 70 KVp, I = 110 µA, increment 7 µm, threshold value = 289 [6,11]. Two hundred slices of the proximal and 33 slices of the midshaft tibia were used for trabecular and cortical bone analysis, respectively. Trabecular bone in vertebrae was measured in the vertebral body after manual exclusion of the superior and inferior end plates, which consisted of approximately 10% of vertebral height on each side.

### Osteoclastogenesis assay

Primary bone marrow cells (PBMC) were harvested as previously described [12], and seeded at the density of  $2.5 \times 10^5/\text{cm}^2$  in the presence of  $\alpha$ -MEM (Invitrogen, Carlsbad, CA) supplemented with 15% FBS (Hyclone, Waltham, MA). Floating, nonadherent cells were harvested after 24 h and seeded at the density of  $2 \times 10^5/\text{cm}^2$  into 48-well plate with the medium supplemented with M-CSF (50 ng/ml) and RANKL (50 ng/ml) (R&D System, Minneapolis, MN). After 4 days of growth, cultures were stained for TRAP5b using the Leukocyte Acid Phosphatase (TRAP<sup>+</sup>) Kit (Sigma). In the coculture experiments, nonadherent PBMC were plated over U-33/γ2 cells, which represent marrow cells of mesenchymal lineage naturally producing RANKL and M-CSF and able to support osteoclastogenesis [11]. U-33/γ2 cells were plated at the density of  $1 \times 10^4/\text{cm}^2$  on 48-well/plate 1 day before nonadherent PBMC were added (at  $2 \times 10^5/\text{cm}^2$ ). Cultures were grown in the media supplemented with  $10^{-8}$  M 1,25-dihydroxy vitamin D<sub>3</sub> for 8 days with media changed on day 4.

### Fluorescence-activated cell sorting (FACS)

Freshly isolated bone marrow was subjected to FACS using FACS-Callibur (BD Pharmingen, Franklin Lakes, NJ) according to the standard protocol. Sorting was performed using following antibodies, CD3-PE (T-cell lineage) (cat #555275), CD11b-FITC (macrophage lineage) (cat #553310), CD45R-APC (B-cell lineage) (cat #553092), and CD16/CD32 (blocking nonspecific binding) (cat #553142), which were purchased from BD Pharmingen. Initial sorting, which excluded cell aggregates and dead cells, was followed by sorting for CD11b. The cell population negative for this antigen was subsequently sorted for both CD3 and CD45R antigens. The population of cells negative for all three antigens (CD11b<sup>-</sup> CD3<sup>-</sup> CD45R<sup>-</sup>) was considered osteoclast precursors [7].

### Analysis of gene expression in mature osteoclasts

Nonadherent marrow cells harvested after 24 h growth of PBMC, as described above, were plated at the density of  $2.5 \times 10^5$  cells/cm<sup>2</sup> in the presence of growth medium ( $\alpha$ -MEM and 15% FBS) supplemented with 50 ng/ml M-CSF. Cells were incubated for 3 days, then received medium supplemented with 50 ng/ml M-CSF and 50 ng/ml RANKL. After additional 3 days of growth, cells were harvested and total RNA isolated using TRIzol reagent (Invitrogen, Carlsbad, CA). Gene expression analysis was performed using real-time PCR (StepOnePlus, Applied Biosystem, Foster City, CA), as previously described [11]. Relative expression was measured by the comparative C<sub>T</sub> method after each sample was normalized to the quantity of 18S RNA. Real-time PCR analysis was performed using previously described primers sets: c-fos, RANK, and M-CSF-R [23], IGF-1 (exon 3 and exon 6) and IGF-1r [13], PPARγ (both isoforms), PPARγ2, Runx2, Dlx5, RANKL, osteocalcin, collagen I and RANKL [11].

### Analysis of marrow mesenchymal cells

To assess the potential of MSC to differentiate toward osteoblasts, PBMC were seeded as a colony forming units type of culture and analyzed as described previously [11]. Gene expression analysis was performed on total RNA isolated from PBMC cultured for 10 days, as described [12]. To assess the effect of insulin on MSC proliferation and alkaline phosphatase activity, PBMC from the wild-type strain were plated on 96-well plates at the density  $1 \times 10^5$  cells/well. Cultures were grown for 10 days either in the absence or presence of insulin (0.1 µM or 1 µM concentration). Cell proliferation was assessed by MTT assay (Promega) and alkaline phosphatase activity was measured and normalized to the cell number, as previously described [12]. Each experiment was repeated three times.

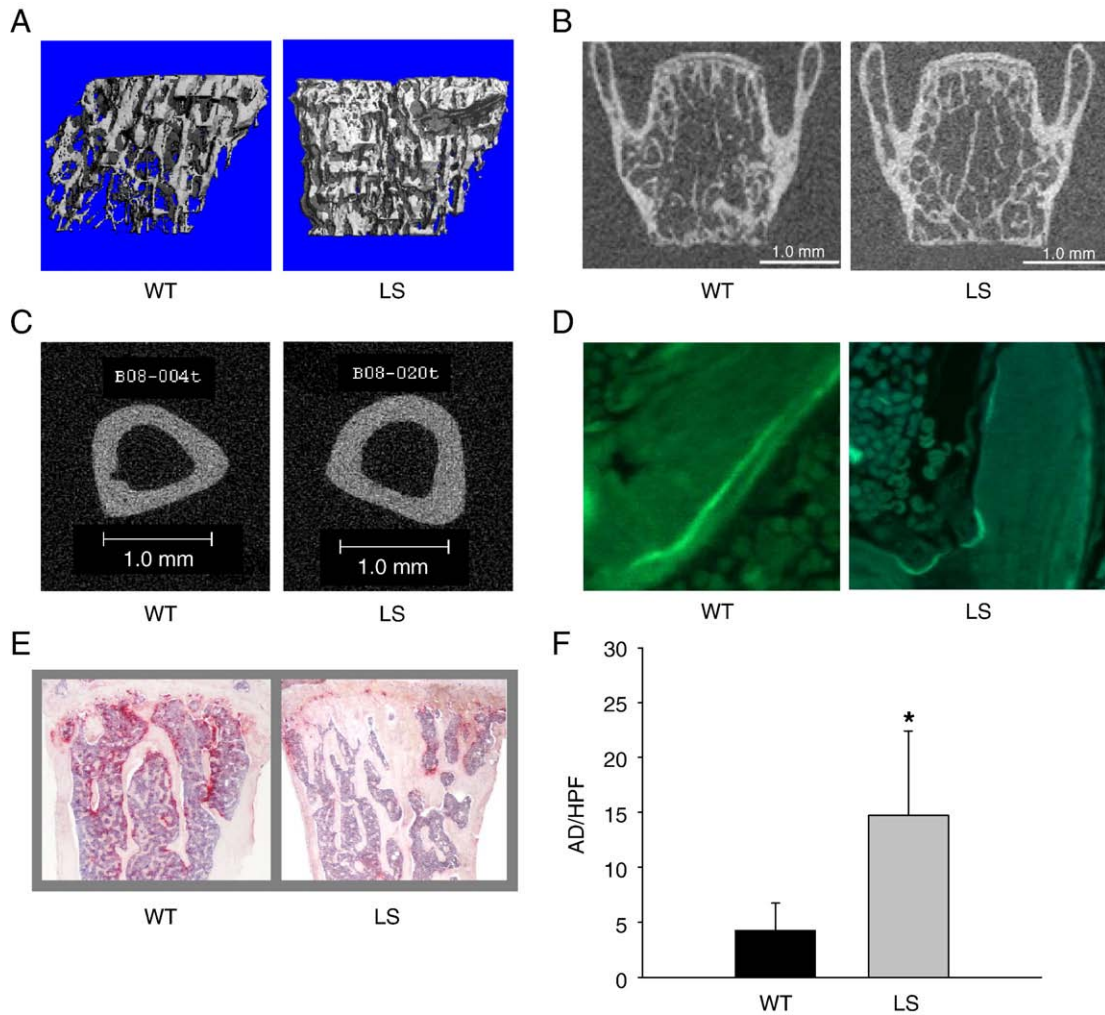


**Fig. 1.** Bone parameters. (A) mCT renderings of trabecular bone in the proximal tibia. (B) mCT-generated coronal section images of L5 vertebral body. (C) Cross-sectional mCT image of tibia metaphysis. (D) Tetracycline-labeled section of the proximal tibia. Tetracycline was injected twice, 7 and 2 days before mouse sacrifice, and the distance between two layers of labeling corresponds to bone formation which occurred during the 5-day period between injections (magnification 40 $\times$ ). (E) Sagittal paraffin section of proximal tibia stained red for TRACP5b and counterstained with Mayer's hematoxylin (magnification 4 $\times$ ). (F) Number of adipocytes (AD) in the proximal tibia calculated per high-power field (HPF) at the magnification 10 $\times$  (\* $p$ <0.05). Adipocytes were identified by their morphologic appearance (empty oval space) in the H&E-stained paraffin sections of bone specimens. The data represent analysis of one experiment; each group consisted of 4 animals. WT indicates wild-type; LS, L-SACC1. (For interpretation of the references to colour in this figure legend, the reader is referred to the web version of this article.)

#### Statistical analysis

Statistical analysis was performed on three independent experiments, each of them consisted of age-matched groups of L-SACC1 and WT animals ( $n=4$  animals per group). Statistically significant differences between groups in each experiment were detected using one-way ANOVA within the SigmaStat software (SPSS, Inc., Chicago, IL). In all cases,  $p<0.05$  was considered significant. Dynamic histomorphometric data were collected from one experiment, 4 animals per group, and differences between parameters determined using ANOVA within the SigmaStat software (SPSS Science, Chicago,

IL). All values are presented as the mean  $\pm$  SD. Differences were considered significant if  $p<0.05$ .

#### Results

##### L-SACC1 mice are hyperinsulinemic, obese and have changes in fat distribution

Consistent with previous reports [17], 5-month-old L-SACC1 males exhibited elevation in body weight ( $30.3 \pm 2.5$  g vs.  $23.5 \pm 2.7$  g;  $p<0.05$ ) with increased visceral fat weight ( $0.874 \pm 0.069$  g vs.

**Table 1**

Trabecular parameters of proximal tibia and vertebrae.

		BV (mm <sup>3</sup> )	BV/TV (%)	Tb. N. (1/mm <sup>2</sup> )	Tb. Th. (mm)	Tb. Sp. (mm)	ConnD (1/mm <sup>3</sup> )	SMI
Prox. tibia	WT <sup>a</sup>	0.20 $\pm$ 0.04	8.1 $\pm$ 0.02	3.43 $\pm$ 0.75	0.022 $\pm$ 0.002	0.279 $\pm$ 0.062	361.7 $\pm$ 105.1	2.6 $\pm$ 0.2
	LS <sup>a</sup>	0.42 $\pm$ 0.05*	14.1 $\pm$ 0.02*	4.94 $\pm$ 0.54**	0.028 $\pm$ 0.002*	0.176 $\pm$ 0.022**	667.6 $\pm$ 181.2**	1.8 $\pm$ 0.2*
Vertebrae	WT <sup>a</sup>	0.12 $\pm$ 0.04	7.9 $\pm$ 0.04	2.83 $\pm$ 1.14	0.021 $\pm$ 0.004	0.366 $\pm$ 0.116	161.8 $\pm$ 167.7	3.2 $\pm$ 0.6
	LS <sup>a</sup>	0.19 $\pm$ 0.0**	10.6 $\pm$ 0.02	3.78 $\pm$ 0.41	0.024 $\pm$ 0.001	0.243 $\pm$ 0.034	297.6 $\pm$ 51.0	2.7 $\pm$ 0.2

All values are expressed as means  $\pm$  SD.

<sup>a</sup>  $n=4$  animals per group.

\*  $p<0.01$  vs. WT.

\*\*  $p<0.05$  vs. WT.

0.321 ± 0.091 g;  $p < 0.05$ ) and decreased interscapular fat mass (0.059 ± 0.024 g vs. 0.093 ± 0.010 g;  $p < 0.05$ ). They also had higher fasting levels of serum insulin (168 ± 51.8 pM vs. 48.5 ± 2.1 pM;  $p < 0.05$ ) and there is no difference in fasting levels of glucose between L-SACC1 and WT animals (103.2 ± 5.3 mg/dl vs. 109.7 ± 7.7 mg/dl). The L-SACC1 animals used in these studies were hyperinsulinemic and obese, but normoglycemic, with changes in fat distribution indicating changes in the energy metabolism.

#### *L-SACC1 mice have increased trabecular and cortical bone mass, decreased bone formation, and decreased number of osteoclasts*

L-SACC1 had higher content of trabecular bone in the tibia and vertebrae as compared to wild-type (WT) mice (Figs. 1A and B, Table 1). The trabecular bone volume (BV/TV) in the tibia was increased by 74% ( $p = 0.0004$ ), connectivity density (ConnD) by 84% ( $p = 0.026$ ), number of trabeculae (TbN) by 44% ( $p = 0.018$ ), and trabeculae thickness (TbTh) by 26% ( $p = 0.008$ ). Consistently, the trabeculae separation (TbSp) was decreased by 37% ( $p = 0.02$ ). The measure of structure model index (SMI) indicated that L-SACC1 trabecular bone architecture was more platelike, in contrast to more rodlike architecture seen in control animals (Fig. 1A and Table 1). Due to large variations between animals, the vertebral measurements did not achieve statistical significance as compared to the control group (Table 1).

Measurements of cortical bone geometry from the midshaft of the tibia showed that L-SACC1 bone had a larger cortical perimeter due to increased cortical area (22.5%;  $p = 0.02$ ) and cortical thickness (11.4%;  $p = 0.03$ ) (Fig. 1C and Table 2). Although being larger and thicker, L-SACC1 bone was not osteopetrotic and had a slightly increased medullary area (8.3%, NS).

Dynamic histomorphometry of the trabecular tibia bone showed attenuated bone formation in L-SACC1 mice (Fig. 1D and Table 3). Assessment of bone formation based on incorporation of tetracycline into newly formed bone shows that only 5% of L-SACC1 bone is active as compared to approximately 70% of WT bone. Due to an insufficient number of double-labeled bone surfaces in L-SACC1 bone evaluations of the mineral apposition rate (MAR) and the bone formation rate (BFR) were not possible (Fig. 1D and Table 3).

The histologic assessment of trabecular bone in the tibia showed a decrease in the number of TRAP-positive osteoclasts in the L-SACC1 bone, as compared to WT (Fig. 1E). The number of adipocytes in the L-SACC1 bone marrow was 3-fold higher than WT (Fig. 1F).

#### *The effects of L-SACC1 mutation on serum bone turnover markers*

Consistent with a lower number of osteoclasts, the levels of bone resorption markers, such as TRAP5b enzyme activity and CTX, a marker of collagen degradation, were significantly lower in serum of L-SACC1 mice (Table 4). The activity of bone-specific alkaline phosphatase was lower in L-SACC1 than in control mice, however the level of P1NP, a marker of collagen production, was higher in L-SACC1 animals (Table 4). Levels of circulating IGF-1 cytokine, which has an anabolic effect on bone, were not different between both strains.

**Table 2**  
Cortical parameters of midshaft of tibia.

	Cross-section area (mm <sup>2</sup> )	Cortical area (mm <sup>2</sup> )	Medullary area (mm <sup>2</sup> )	Cortical thickness (mm)
WT <sup>a</sup>	0.203 ± 0.017	0.127 ± 0.009	0.076 ± 0.009	0.184 ± 0.011
LS <sup>a</sup>	0.238 ± 0.029	0.155 ± 0.016*	0.083 ± 0.015	0.205 ± 0.011*

All values are expressed as means ± SD.

<sup>a</sup> n = 4 animals per group.

\*  $p < 0.05$  vs. WT.

**Table 3**  
Dynamic histomorphometry of L-SACC1 (LS) and wild-type (WT) tibia trabecular bone.

	Single-labeled surface/BS (%)	Double-labeled surface/BS (%)	Nonlabeled surface (%)	MAR (μm/d)	BFR/BS (μm <sup>3</sup> /μm <sup>2</sup> /d)
WT	14.2 ± 11.1	61.4 ± 9.2	35.4 ± 7.7	0.75 ± 0.03	0.27 ± 0.05
LS	4.3 ± 3.5*	1.4 ± 1.0*	94.3 ± 2.2*	ND	ND

Values are expressed as means ± SD of n = 4 animals per group. BS indicates bone surface; MAR, mineral apposition rate; BFR, bone formation rate; ND, not detected.

\*  $p < 0.001$  L-SACC1 vs. WT.

#### *Reduced number and impaired differentiation of osteoclast precursors from L-SACC1 mice*

FACS analysis of freshly isolated bone marrow showed that the lineage distribution of myelopoietic cells in L-SACC1 and WT marrow is different. The number of osteoclast precursors, measured as a pool of cells negative for CD11b, CD3, and CD45R, was 40% lower in L-SACC1 than WT mice (Table 5). The number of CD45<sup>+</sup> cells, which represent B-cell precursors, was increased by 60%. No differences in the number of cells positive for CD11b (macrophage marker) and CD3 (T-cell marker) were observed (Table 5).

To further address the issue of decreased osteoclastogenesis observed in L-SACC1 mice, we compared the efficiency of osteoclast recruitment from the pool of hematopoietic cells and their differentiation potential toward osteoclasts in the presence of either an excessive amount of exogenously added RANKL and M-CSF cytokines, or a limited supply of these cytokines such as coculturing with U-33/γ2 cells [11,14]. The number of TRAP<sup>+</sup> osteoclastlike cells in L-SACC1 was lower by 40% when cultured in the presence of exogenously added cytokines (Fig. 2A), and by 20-fold when the cytokines supply was limited (Fig. 2B). The more marked reduction in TRAP<sup>+</sup> cells in the condition of limited cytokine supply indicates impairment in differentiation potential of existing osteoclast precursors. Moreover, there was a notable difference in the maturation of TRAP<sup>+</sup> cells in both conditions, with those from WT nonadherent cells being more mature (appearing large and possessing multiple nuclei) than the majority of TRAP<sup>+</sup> cells from L-SACC1 precursors which were smaller and possessed a low number of nuclei (Fig. 2C).

Analysis of the expression of genes essential for intrinsic regulation of osteoclastogenesis showed that osteoclast precursors from L-SACC1 animals expressed lower levels of c-fos and RANK gene transcripts (Fig. 2D). Products of these genes are essential for RANKL signaling and osteoclast differentiation [3]. The level of receptors for other osteoclast-supporting factors, M-CSF and IGF-1, was not different between L-SACC1 and WT animals. Similarly, transcript levels for PPARγ nuclear receptor, which has been recently identified as a transcriptional regulator of c-fos and RANK expression in osteoclasts [23], was not altered (data not shown).

#### *Insulin decreased osteoclastogenesis and the expression of c-fos and RANK in nonadherent PBMC*

Since L-SACC1 animals have elevated circulating levels of insulin, we tested the effect of insulin on WT-derived osteoclast differentiation

**Table 4**  
Serum bone turnover markers.

	WT <sup>a</sup>	L-SACC1 <sup>a</sup>	p value
TRAP5b (U/L)	0.428 ± 0.073	0.216 ± 0.068	0.005
CTX (ng/ml)	15.60 ± 2.48	10.33 ± 3.50	0.05
BALP (μU/min)	0.026 ± 0.003	0.014 ± 0.002	0.0003
P1NP (ng/ml)	1.44 ± 0.37	2.09 ± 0.25	0.03
IGF1 (ng/ml)	296.3 ± 30.9	297.3 ± 34.0	0.967

TRAP5b indicates tartrate-resistant acid phosphatase form 5b; CTX, C-terminal telopeptide of type I collagen; BALP, bone-specific alkaline phosphatase; P1NP, N-terminal propeptide of type I procollagen; IGF1, insulinlike growth factor 1.

<sup>a</sup> n = 4 animals per group, 3 experiments.

**Table 5**  
FACS analysis of primary bone marrow cells.

	OCP (CD3 <sup>-</sup> CD11b <sup>-</sup> CD45R <sup>-</sup> )	Macrophage (CD11b <sup>+</sup> )	B cell (CD3 <sup>-</sup> CD11b <sup>-</sup> CD45 <sup>+</sup> )	T cell (CD3 <sup>+</sup> CD11b <sup>-</sup> CD45R <sup>-</sup> )
WT <sup>a</sup>	12.48 ± 3.09	33.23 ± 5.27	15.3 ± 5.04	2.3 ± 0.22
LS <sup>a</sup>	7.9 ± 1.1*	32.23 ± 1.78	24.13 ± 1.83*	2.0 ± 0.14

All values are expressed as means ± SD and represent a percent of sorted PBMC. OCP indicates osteoclast progenitors.

<sup>a</sup> n = 4 animals per group.

\* p < 0.05 vs. WT.

and osteoclast-specific gene expression *in vitro*. As shown in Fig. 3A, an addition of insulin to the ex vivo osteoclast cell cultures affected the number of TRAP<sup>+</sup> cells and their multinucleation. In the presence of 0.1 μM insulin the number of TRAP<sup>+</sup> cells was decreased by 40% (Fig. 3B) and the number of multinucleated TRAP<sup>+</sup> cells was reduced by 20% (Fig. 3C). Interestingly, in the presence of 1 μM insulin the number of TRAP<sup>+</sup> cells was decreased by 50% (Fig. 3B), while the number of multinucleated cells was reduced by more than 90% (Fig. 3C). These results are consistent with *in vivo* findings and indicate that insulin affects both, recruitment and osteoclasts differentiation, however by different mechanisms which are determined by the dose of insulin in *in vitro* conditions.

An analysis of gene expression showed that insulin affects the expression of c-fos and RANK but not M-CSF and IGF-1 receptors (Fig. 3D). This change of gene expression by insulin *in vitro* is identical to that of osteoclasts derived from L-SACC1 animals.

#### The effects of L-SACC1 mutation and insulin on mesenchymal stem cell (MSC) phenotype

The differentiation potential of MSC toward osteoblasts and adipocytes was measured in CFU-OB and CFU-AD type of culture,

respectively, and was not different between L-SACC1 and WT animals (data not shown). Similarly, mRNA levels of osteoblast-specific genes for Runx2, Dlx5, RANKL, osteocalcin and collagen I, were not different in MSCs isolated from L-SACC1 and WT animals (data not shown). Although the levels of circulating IGF-1 were not different (Table 4), however the expression of the bone-specific long transcript for IGF-1 was decreased and that of PPARγ2, an adipocyte-specific transcription factor, was increased in MSC of L-SACC1 animals (Fig. 4A). Increased expression of PPARγ2 correlates with the increased number of adipocytes in the marrow of L-SACC1 mice (Fig. 1G). Ex vivo analysis of insulin effects on PBMC showed that, at the tested doses, insulin neither affected MSC proliferation (Fig. 4B) nor MSC alkaline phosphatase activity (Fig. 4C).

#### Discussion

The current studies present evidence for an importance of efficient hepatic insulin clearance in the maintenance of bone homeostasis. In the L-SACC1 murine model we have shown that impaired insulin clearance in the liver, which results in high levels of circulating insulin and insulin resistance in peripheral tissues, leads to decreased bone turnover. It affects bone remodeling process by decreasing both, bone

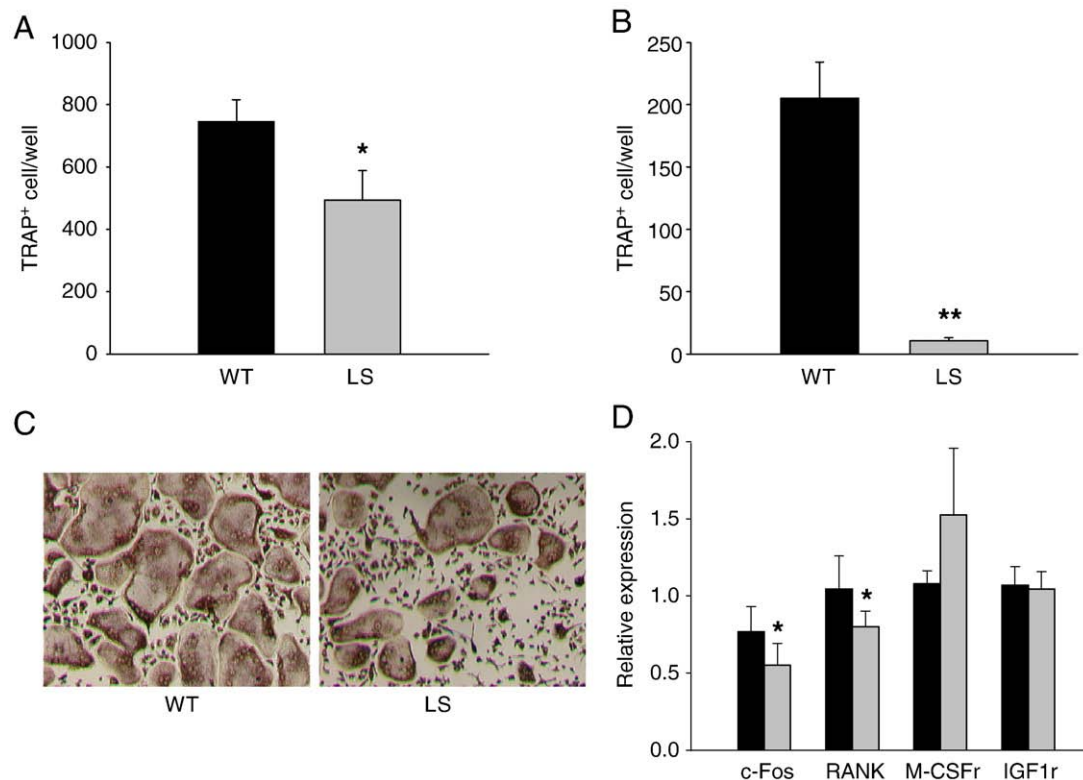


**Fig. 2.** Osteoclast differentiation of nonadherent marrow cells derived from L-SACC1 (LS) and wild-type (WT) animals. (A) Number of TRAP<sup>+</sup> cells developed from nonadherent marrow cells after 4 days of culture in the presence of M-CSF (50 ng/ml) and RANKL (50 ng/ml). (B) Number of TRAP<sup>+</sup> cells developed from nonadherent marrow cells cocultured with U-33/γ2 cells to support osteoclastogenesis. (C) Appearance of TRAP<sup>+</sup> osteoclastlike cells developed in the culture supplemented with M-CSF and RANKL. (D) Real-time PCR analysis of gene expression in osteoclastlike cells after 4 days of culture in the presence of M-CSF and RANKL. Filled bars (black—WT, gray—LS) represent means of 4 samples corresponding to 4 different animals per group. The experiment was repeated 3 times. Vertical bars represent SD. \*p < 0.05. \*\*p < 0.05.

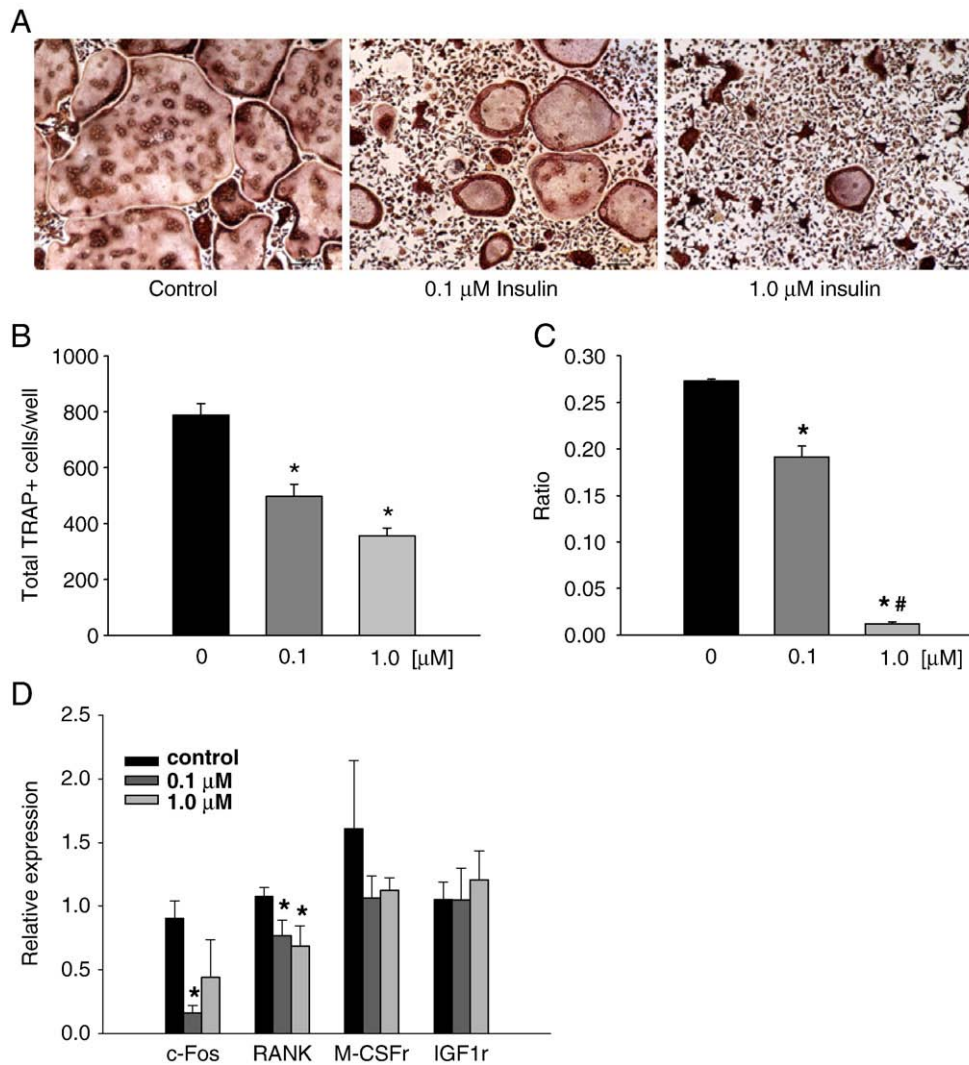


**Fig. 3.** *In vitro* analysis of insulin effects on osteoclast differentiation and gene expression. Nonadherent marrow cells were derived from WT animals ( $n = 4$ ) and cultured separately as described in **Materials and methods**. The experiment was repeated 3 times. (A) An appearance of TRAP<sup>+</sup> osteoclastlike cells after 4 days of culture in the presence of M-CSF and RANKL and insulin at different concentrations. (B) Calculated number of TRAP<sup>+</sup> cells. (C) The ratio of multinucleated TRAP<sup>+</sup> cells (more than 3 nuclei) to the total TRAP<sup>+</sup> cells. (D) The effect of insulin on gene expression in osteoclastlike cells developed as in (A) and analyzed by real-time PCR. \* $p < 0.05$  vs. control; # $p < 0.05$  vs. 0.1  $\mu\text{M}$  insulin.

formation and bone resorption. It also changes myelopoietic cell commitment toward the osteoclast and B-cell lineages. We have demonstrated in both, *in vivo* and *in vitro* systems, that high levels of insulin affect recruitment and differentiation of osteoclasts by impairing the RANKL signaling pathway. In osteoclasts, expression of the RANK receptor is under the control of the c-fos transcription factor [1], and insulin modulates the expression of both genes. Using PBMC derived from normoinsulinemic animals, we showed that exogenously added insulin affects osteoclast differentiation and the expression of RANK and c-fos in a manner identical to L-SACC1 animals. These findings provide evidence that insulin negatively regulates the phenotype of cells of the osteoclast lineage, and suggest that systemic hyperinsulinemia has a permanent effect on osteoclast progenitors.

The effect of insulin on cells of mesenchymal lineage is less evident. Differentiation potential of MSCs derived from L-SACC1 animals toward osteoblast lineage and the expression of osteoblast gene markers were not different from MSCs derived from WT animals, with exception to IGF-1 which expression was decreased. In contrast to studies of other's [4,21], insulin neither increase alkaline phosphatase activity nor cell proliferation when added to the PBMC culture. However, serum parameters of bone formation in L-SACC1 were

significantly different from that of WT animals. These data suggest that systemic changes, which result from CEACAM1 mutation in the liver, affect osteoblast function in the bone in an indirect manner, which does not involve intrinsic changes in MSC differentiation potential. In contrast to cells of hematopoietic lineage, *in vitro* effect of insulin on MSC osteoblast phenotype does not recapitulate attenuated bone formation in L-SACC1 animals, suggesting that CEACAM1 mutation in the liver affects marrow mesenchymal cells by different mechanism than cells of hematopoietic lineage.

We have reported previously that PPAR $\gamma$ 2, an adipocyte-specific transcription factor, suppresses the expression of IGF-1 in bone, especially its longer isoform which contains exon 6 [13]. Here, we showed that L-SACC1 mice are characterized by increased expression of PPAR $\gamma$ 2 in marrow MSC. Thus, PPAR $\gamma$ 2 may be responsible for decreased IGF-1 expression. Interestingly, although we did not observe an increase in CFU-AD formation in *ex vivo* conditions, L-SACC1 animals possess higher number of adipocytes in the bone marrow. The discrepancy between *ex vivo* and *in vivo* observation indicate that in *in vivo* conditions, an additional factor, perhaps insulin, which possesses proadipocytic activity [27], enhanced adipocytic differentiation of MSC. Taken together, these results suggest that prolonged exposure to high levels of insulin induces

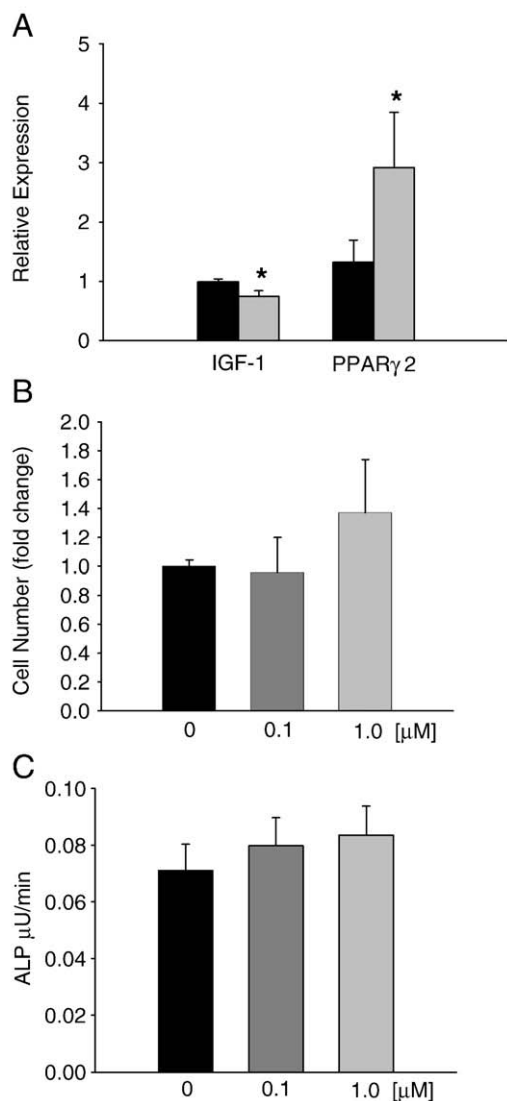


**Fig. 4.** The effect of the L-SACC1 mutation and insulin on marrow MSC phenotype. (A) The PPAR $\gamma$ 2 and IGF-1 gene expression in MSC derived from WT (black bars) and LS (gray bars) animals (n = 4 animals per group). (B) The *in vitro* effect of insulin on MSC proliferation. (C) The *in vitro* effect of insulin on alkaline phosphatase activity in MSC. The MSC were derived from bone marrow of WT animals (n = 4) and assayed as 4 separate cell isolates. The experiment was repeated 3 times. \*p < 0.05; \*\*p < 0.01.

the adipocyte phenotype in MSC and decreases the expression of IGF-1, a positive regulator of osteoblast function [19], which may contribute to the decreased bone formation rate observed in L-SACC1 animals.

Several studies point toward a decreased bone turnover rate in T2DM [2,9]. An analysis of serum bone turnover parameters in T2DM patients and in diabetic Pima Indians showed reduced bone formation, as assessed by low levels of alkaline phosphatase, osteocalcin and IGF-1 [2]. Another study based on longitudinal observations of bone status showed attenuation of the rate of bone loss with aging and relatively higher bone mass in T2DM patients [9]. The higher bone mass in L-SACC1 animals is entirely consistent with low bone turnover, which results from attenuated bone resorption and decreased bone formation.

A paradox between normal or higher BMD and increased fracture risk in T2DM suggests altered quality in diabetic bone. In addition to hyperinsulinemia leading to low bone turnover, hyperglycemia may account for changes in bone biomaterial quality by modification of collagen fibers [18]. Highly reactive glucose metabolites (AGEs), of

which circulating levels are increased in diabetic hyperglycemia, are implicated in forming cross-links between collagen fibers, which affect bone biomechanical properties by increasing its stiffness and fragility [22,26].

Using the L-SACC1 model of hyperinsulinemia caused by liver-specific impairment in insulin clearance, we have demonstrated that high insulin levels affect bone resorption and impair bone formation, leading to a decreased bone turnover rate. Because altered insulin action in L-SACC1 mice is primarily hepatic, our studies suggest that insulin metabolism in the liver, which regulates overall insulin action in peripheral tissues (muscle and adipose tissue) [16], regulates also the maintenance of bone mass. The similarity of the phenotype of L-SACC1 mice with hyperinsulinemia in humans emphasizes the relevance of the current studies in advancing our understanding of the altered bone homeostasis in diabetes.

#### Acknowledgments

We thank Dr. L. Suva for dynamic histomorphometry analysis. This work was supported by the following funds: BLC–NIH/NIA AG 028935; American Diabetes Association's Amaranth Diabetes Fund 1–09–RA–95; MFM–USDA 38903–02315; SMN–NIH/NIDDK DK 54254; and USDA 38903–02315.

#### References

- Asagiri M, Takayanagi H. The molecular understanding of osteoclast differentiation. *Bone* 2007;40:251–64.
- Bouillon R, Bex M, Van Herck E, Laureys J, Doooms L, Lesaffre E, et al. Influence of age, sex, and insulin on osteoblast function: osteoblast dysfunction in diabetes mellitus. *J Clin Endocrinol Metab* 1995;80:1194–202.
- Boyce BF, Xing L. Functions of RANKL/RANK/OPG in bone modeling and remodeling. *Arch Biochem Biophys* 2008;473:139–46.
- Canalis E. Effect of hormones and growth factors on alkaline phosphatase activity and collagen synthesis in cultured rat calvariae. *Metabolism* 1983;32:14–20.
- DeAngelis AM, Heinrich G, Dai T, Bowman TA, Patel PR, Lee SJ, et al. Carcinoembryonic antigen-related cell adhesion molecule 1: a link between insulin and lipid metabolism. *Diabetes* 2008;57:2296–303.
- Holdsworth DW, Thornton MM. Micro-CT in small animal and specimen imaging. *Trends Biotechnol* 2002;20:S34–9.
- Jacquin C, Gran DE, Lee SK, Lorenzo JA, Aguila HL. Identification of multiple osteoclast precursor populations in murine bone marrow. *J Bone Miner Res* 2006;21:67–77.
- Janghorbani M, Van Dam RM, Willett WC, Hu FB. Systematic review of type 1 and type 2 diabetes mellitus and risk of fracture. *Am J Epidemiol* 2007;166:495–505.
- Krakauer JC, McKenna MJ, Buderer NF, Rao DS, Whitehouse FW, et al. Bone loss and bone turnover in diabetes. *Diabetes* 1995;44:775–82.
- Kuespert K, Pils S, Hauck CR. CEACAMs: their role in physiology and pathophysiology. *Curr Opin Cell Biol* 2006;18:565–71.
- Lazarenko OP, Rzonca SO, Hogue WR, Swain FL, Suva LJ, et al. Rosiglitazone induces decreases in bone mass and strength that are reminiscent of aged bone. *Endocrinology* 2007;148:2669–80.
- Lazarenko OP, Rzonca SO, Suva LJ, Lecka-Czernik B. Netoglitazone is a PPAR-gamma ligand with selective effects on bone and fat. *Bone* 2006;38:74–85.
- Lecka-Czernik B, Ackert-Bicknell C, Adamo ML, Marmolejos V, Churchill GA, Shockley KR, et al. Activation of peroxisome proliferator-activated receptor gamma (PPARgamma) by rosiglitazone suppresses components of the insulin-like growth factor regulatory system in vitro and in vivo. *Endocrinology* 2007;148:903–11.
- Lecka-Czernik B, Gubrij I, Moerman EA, Kajkenova O, Lipschitz DA, Manolagas SC, et al. Inhibition of Osf2/Cbfa1 expression and terminal osteoblast differentiation by PPAR-gamma 2. *J Cell Biochem* 1999;74:357–71.
- Najjar SM. Regulation of insulin action by CEACAM1. *Trends Endocrinol Metab* 2002;13:240–5.
- Park SY, Cho YR, Kim HJ, Hong EG, Higashimori T, Lee SJ, et al. Mechanism of glucose intolerance in mice with dominant negative mutation of CEACAM1. *Am J Physiol Endocrinol Metab* 2006;291:E517–24.
- Poy MN, Yang Y, Rezaei K, Fernstrom MA, Lee AD, Kido Y, et al. CEACAM1 regulates insulin clearance in liver. *Nat Genet* 2002;30:270–6.
- Reinwald S, Peterson RG, Allen MR, Burr DB. Skeletal changes associated with the onset of type 2 diabetes in the ZDF and ZSD rodent models. *Am J Physiol Endocrinol Metab* 2009;296:E765–74.
- Rosen CJ. Insulin-like growth factor I and bone mineral density: experience from animal models and human observational studies. *Best Pract Res Clin Endocrinol Metab* 2004;18:423–35.
- Thomas DM, Udagawa N, Hards DK, Quinn JM, Moseley JM, Findlay DM, et al. Insulin receptor expression in primary and cultured osteoclast-like cells. *Bone* 1998;23:181–6.

- [21] Thrailkill KM, Lumpkin Jr CK, Bunn RC, Kemp SF, Fowlkes JL. Is insulin an anabolic agent in bone? Dissecting the diabetic bone for clues. *Am J Physiol Endocrinol Metab* 2005;289:E735–45.
- [22] Vashishth D. Collagen glycation and its role in fracture properties of bone. *J Musculoskelet Neuronal Interact* 2005;5:316.
- [23] Wan Y, Chong LW, Evans RM. PPAR-gamma regulates osteoclastogenesis in mice. *Nat Med* 2007;13:1496–503.
- [24] White MF. Insulin signaling in health and disease. *Science* 2003;302:1710–1.
- [25] Xu E, Dubois MJ, Leung N, Charbonneau A, Turbide C, Avramoglu RK, et al. Targeted disruption of carcinoembryonic antigen-related cell adhesion molecule 1 promotes diet-induced hepatic steatosis and insulin resistance. *Endocrinology* 2009;150:3503–12.
- [26] Yamamoto M, Yamaguchi T, Yamauchi M, Yano S, Sugimoto T. Serum pentosidine levels are positively associated with the presence of vertebral fractures in postmenopausal women with type 2 diabetes. *J Clin Endocrinol Metab* 2008;93:1013–9.
- [27] Zhang HH, Huang J, Duvel K, Boback B, Wu S, Squillace RM, et al. Insulin stimulates adipogenesis through the Akt-TSC2-mTORC1 pathway. *PLoS One* 2009;e6189:4.